

Synthesis of Mesoporous Silica from Palm Oil Boiler Ash (MS-POBA) with Addition of Methyl Ester Sulfonate as a Template for Free Fatty Acid Adsorption from Crude Palm Oil (CPO)

Cita Sitohang, Agus Kuncaka, and Adhitasari Suratman*

Department of Chemistry, Faculty of Mathematics and Natural Sciences, Universitas Gadjah Mada, Sekip Utara, Yogyakarta 55281, Indonesia

* **Corresponding author:**

tel: +62-85878677591

email: adhitasari@ugm.ac.id

Received: August 6, 2023

Accepted: February 20, 2024

DOI: 10.22146/ijc.87703

Abstract: The synthesis of mesoporous material by utilizing palm oil boiler ash (POBA) waste as the silica source and methyl ester sulfonate (MES) surfactant as the template for a high-porosity was investigated for free fatty acids (FFA) adsorption. The research was initiated with silica extraction from POBA by sodium hydroxide addition through the sol-gel precipitation method. Silica modification was carried out with MES surfactant and 3-aminopropyltrimethoxysilane (APTMS) as the co-structure-directing agent (CSDA) in different calcination temperatures. Mesoporous silica-POBA (MS-POBA) free template had a surface area, pore diameter, and pore volume ($41.033 \text{ m}^2/\text{g}$, 4.180 nm , and $0.250 \text{ cm}^3/\text{g}$) lower than MS-POBA with the template ($71.0147 \text{ m}^2/\text{g}$, 7.923 nm , and $0.524 \text{ cm}^3/\text{g}$). The ability of MS-POBA to adsorb FFA reached its optimum conditions with an adsorption time of 20 min and an adsorbent dosage of 0.24 g. The FFA removal by MS-POBA with the template was found to have higher adsorption ability, which was 35.54%, compared to the MS-POBA free template of 26.68%. The high porosity of MS-POBA with a template makes the FFA adsorption capacity of this material higher than MS-POBA free template.

Keywords: silica; surfactant; MES; FFA

■ INTRODUCTION

Indonesia is one of the world's largest palm oil plantations, covering an area of 14.09 million hectares, and it holds the title of the largest palm oil producer globally with dominance in Sumatra and Kalimantan [1-2]. Crude palm oil (CPO) is a primary product of palm oil mills. Processing CPO from palm oil in the industry produces a lot of solid waste, such as 23% empty fruit bunches, where 15% in the form of fiber and the other 6% in the form of shells, while they are used to generate electricity in the industry palm oil mill from the steam-driven turbine. Palm oil boiler ash (POBA) is an environmental problem because it is a waste of the palm oil mill industry. POBA is ash derived from shells and fruit fiber that have been ground and burned at a temperature of 500 to 700 °C in a boiler furnace and it contains silica chemical elements such as SiO_2 (49.50%), Al_2O_3 (5.45%), and Fe_2O_3 (5.73%) [3-6].

Silica from boiler ash is obtained through a synthesis process using the sol-gel method by adding sodium hydroxide, where 37% of silica is obtained [7-9]. Apart from the purity, the important thing about silica is the presence of porous silica. The pore diameter size of silica, according to the International Union of Pure and Applied Chemistry (IUPAC) is classified into micropores (pore size below 2 nm), mesoporous (pore size between 2 to 50 nm), and macropores (pore size above 50 nm). The details about porosity, density, specific surface area or pore size, and pore size distribution in porous solids depend on the adsorbate that enters the pore gaps. The results are influenced by the size of the molecule that is passed through the pores [10].

The properties of silica are affected by particle size, pore size, pore volume, and surface characteristics of the material [11]. Several methods can be utilized to form

nanoparticles, such as thermal decomposition, microemulsions, co-precipitation, sol-gel, and hydrothermal. Silica can be modified by organic ligands [12-13] and additional surfactants (categorized as cationic, anionic, and non-ionic) as a template since it is more attractive and commonly used due to the presence of a hydrophobic tail and a hydrophilic head. An appropriate surfactant required for modifications might be different depending on the nature of adsorbents and adsorbate interactions.

Anionic surfactants have also been widely used, including sodium dodecyl sulphate (SDS), sodium dodecyl benzene sulfonate (SDBS), and sodium ricinoleate [14-18]. The most relevant surfactant required for modification depends on the nature of the adsorbent and the interactions of the adsorbate [19]. The previous work modified mesoporous silica nanoparticles by varying the molar ratio of two anionic surfactants [18] and this research used only one anionic surfactant. Methyl ester sulfonate (MES), a kind of anionic surfactant derived from palm oil, has good surface-active properties and has recently been named a green surfactant [20]. These compounds include new surfactants, which are renewable resources (from renewable materials) and are biodegradable because they are made from vegetable oils and can be produced economically.

There has not been any research on the use of this MES surfactant as a template in the synthesis of mesoporous silica materials, which is based on the literature that was found. This MES anionic surfactant has the chemical formula $RCH(CO_2Me)SO_3Na$. Its carbon chain contains a double bond (C9 atom) and a hydroxy group (C7 atom); both might influence the formation of micelle aggregates and consequently affect the porous characteristics of mesoporous silica. It has been discovered that the co-structure-directing agent (CSDA)/surfactant ratio, alkyl chain length, and surfactant ionization level all affect the size of silica pores [15]. The hydrophobic interactions between the organic groups of CSDA on the silica wall and the hydrophobicity of the micelles drive the formation of mesopores [21].

The increase in the pore size of boiler ash silica using MES as a template is interesting. Mesoporous silica palm

oil boiler ash (MS-POBA) was prepared using a simple microemulsion polymerization method and then used as an adsorbent. MES, which was initially used as a template agent during synthesis, was retained in a silica framework, and the product of the synthesis was denoted as MES silica nanoparticles. Mesoporous silica has been used as an adsorbent [13,22-23] and this study aims to reduce free fatty acid (FFA) in CPO by adsorption process. CPO quality standards in Indonesia refer to SNI 01-2901-2006. Under this regulation, tradeable CPO has a FFA content of less than 5%. The higher FFA production is due to enzyme activities in the fruits, from which microbial lipases produce Kerner and react with oil and water during the storage process through hydrolysis of the triglyceride component. The MS-POBA with the template provided active sites and porosity to enhance the FFA adsorption performance. Evaluation of the MS-POBA with the template in adsorbing FFA from CPO was conducted using batch adsorption. An experimental study on the adsorbent dose and contact time effects for FFA was performed.

■ EXPERIMENTAL SECTION

Materials

POBA as a silica bio-source from Riau, Indonesia and CPO from PTKI Medan. Sodium hydroxide (NaOH, 99%), hydrochloric acid (HCl, 37%), MES as a surfactant were purchased from Rendychem. APTMS, ethanol 96%, phenolphthalein, methanol, other chemicals, and solvents were produced from Merck and Sigma Aldrich in pro-analytical grade and used without further purification.

Instrumentation

The instrumentation used for the characterization in this study includes X-ray diffraction (XRD-600, Shimadzu), which is measured by using an 18 kW diffractometer with monochromated $CuK\alpha$ radiation and with scattering reflections recorded for 2θ angles corresponding to d-spacing. Fourier-transform infrared spectroscopy (FTIR, Prestige-21 Shimadzu) in the range $400-4000\text{ cm}^{-1}$ was performed using the standard KBr pellet technique. The equipment used in this research consisted of a furnace, reflux equipment, a magnetic

stirrer, and pH meters. The specific surface area was determined using the surface area analyzer Brunauer-Emmett-Teller (Gemini VII Version 5.03, Micromeritic) method from the adsorption data in the relative pressure range (P/P_0) by a micromeritics. The morphological compositions were analyzed using field emission scanning electron microscopy with energy disperse X-ray (SEM-EDX, JSM-6510).

Procedure

Synthesis of the silica from boiler ash palm oil

As much as 100 g of POBA was refluxed in 200 mL of 6 M HCl solution at 120 °C for 3 h at a speed of 250 rpm and then washed using distilled water at neutral pH conditions. The solid was then dried at 120 °C for 3 h and was calcined at 750 °C for 3 h [24]. For the preparation of sodium silicate solution, 10 g of POBA was entirely dissolved in NaOH solution, then boiled and stirred for 1 h and filtered [25]. The filtrate was added with HCl 2 M until it reached pH 7 then the solution was left at room temperature for 18 h for aging. The solution was filtered and washed with distilled water to remove excess acid to achieve a neutral pH [9] and then before calcination at 500 °C for 4 h, the solution was dried at 90 °C for 12 h.

Synthesis of the silica with template MES

To synthesize the MS-POBA MES template, 2.7 mmol of MES as a template was first added to deionized water, and HCl 0.1 M in a round-bottomed glass flask at 40 °C for 1 h (solution A). In a different beaker glass was weighed 2.4 g (40 mmol) of SiO₂ and APTMS 9.6 mmol were mixed in a 250 mL glass flask and then dissolved in methanol (solution B). Solution B was dropped into solution A and was shaken at 250 rpm speed and sufficient contact time of 1 h. The solution was refluxed at 70 °C for 5 h and washed using distilled water at neutral pH conditions. The product was heated at 70 °C for 5 h and then calcined at 550, 750, and 950 °C for 4 h.

Adsorption experiments

Adsorption experiments were carried out in batch conditions. The FFA levels were determined by SNI 01-2901-2006. Typically, preheated CPO 50 °C was weighed, and dissolved in 50 mL neutral ethanol; as well as two drops of 1% phenolphthalein indicator. Titration was

performed using 0.103 M NaOH solution in deionized water until it turned orange in color. The FFA (%) was calculated based on the Eq. (1):

$$\%FFA = \frac{v \text{ NaOH} \times M \text{ NaOH} \times 25.6}{w} \times 100\% \quad (1)$$

where %FFA represents the percentage of FFA, M is the NaOH concentration (0.103 M), v represents the amount of NaOH in volume (mL), and w represents the weight of CPO (g).

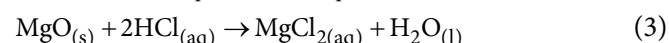
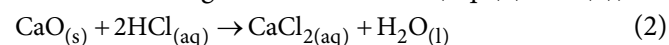
Parameter optimization of adsorption FFA by MS-POBA

The application silica of boiler ash with template MES using mass variation (adsorbent dose) of MS-POBA (0.08, 0.12, 0.16, 0.20, 0.24, and 0.28 g), then mixed with 5 g of CPO. Furthermore, observations were made at the adsorbent contact time for 5, 10, 15, and 20 min, stirrer speed of 300 rpm with heating of 50 °C.

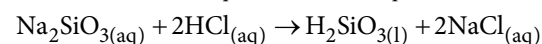
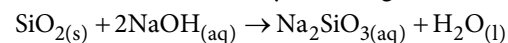
RESULTS AND DISCUSSION

Synthesis of the Silica from Palm Oil Boiler Ash

The sample is first prepared by sieving it on a sieve with a 120-mesh sieve. The presence of metal oxides other than silica contained in the ashes of palm oil mill boilers, such as metal oxides of iron, calcium, and magnesium, can be purified by the addition of HCl. Some reactions occur in the metals contained in the ashes with strong acids such as HCl (Eq. (2) and (3)).



The silica extraction process of POBA in 6 M NaOH produced a sodium silicate solution. Sodium silicate was added with 6 M HCl by the sol-gel method at pH 7.



The sol-gel precipitate was then separated by the filtration method. The precipitate was dried to release its water content and formed silica powder, as shown in Eq. (4). Based on the research that has been carried out, the results of silica extraction from 10 g of boiler ash obtained a silica yield percentage of 44.6% or if it converts into the mass of silica produced 4.46 g.

Synthesis of the Silica with Template MES

The interaction between organic (surfactants) and inorganic (silica oligomers) species has been considered an important variable in the formation of mesoporous materials. To maintain these interactions, several synthesis techniques are necessary for various types of surfactants. CSDA was initially introduced into the anionic surfactant templating system since under acidic conditions, anionic surfactant could be substantially protonated, whereas, under alkaline conditions, the interactions of counter-cations with surfactant and silicate ions are relatively weak. A type of CSDA is an amino silane group, such as APTMS [16]. The electrostatic interaction between the positively charged ammonium sites of CSDAs and the negatively charged headgroups of anionic surfactants is what propels the development of highly structured mesostructures.

The addition of HCl can liberate Na^+ from sodium MES to form SO_4^- and protonate the amine group (NH_2) from APTMS to become NH_3^+ . The interaction between

the MES template and APTMS is getting better because all the SO_4^- groups from MES and the NH_3^+ groups from APTMS are involved in electrostatic interactions, which will determine the porous nature of the silica material. Free template silica and APTMS were dissolved in methanol. Methanol serves as a co-solvent to homogenize the reaction. The addition of methanol can affect the packing of the methyl ester sulfonate template, which functions as a pore former. The schematic strategy of the synthesis of the MS-POBA MES template materials product is shown in Fig. 1.

Tetraalkoxysilane and the CSDA's alkoxy silane groups interact to produce the silica framework after co-condensing. The silicon atoms are covalently bound to the cationic ammonium groups by trimethylene groups of APTMS. This innovative approach succeeds in generating a variety of structures. By using the calcination process, the anionic surfactant templates were eliminated. The MS-POBA was then calcined at temperatures ranging from 550, 750, and 950 °C.

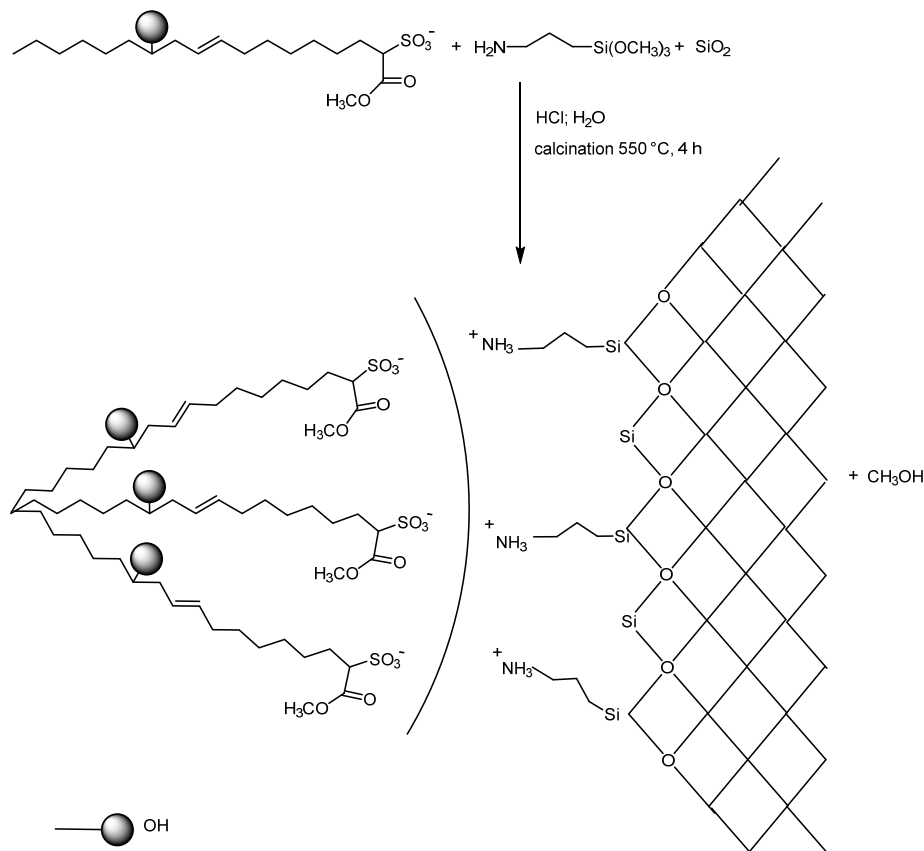


Fig 1. The illustration of the interaction between SiO_2 with MES

FTIR Data

FTIR analysis is a tool used for quantitative analysis based on existing functional groups using standards KBr. Based on Fig. 2, the broadening absorption at wavenumber 3448 cm^{-1} indicates the presence of stretching vibrations of the $-\text{OH}$ (Si-OH), and wavenumber $802\text{--}1103\text{ cm}^{-1}$ indicates asymmetric Si-O-Si vibrations.

The sulfonate groups in MES samples can be seen at the peak at wavenumbers $1226\text{ to }1126\text{ cm}^{-1}$ and the S=O group at wavenumber 1049 cm^{-1} . The formation of sulfonate groups (SO_3), i.e., S=O and S-O stretching absorption bands, was observed at wavenumbers of 1006 and 902 cm^{-1} [26]. Based on Fig. 2(a), it can be seen that the absorption at 1080 and 1226 cm^{-1} indicates the presence of symmetric and asymmetric group strain vibrations. The shift in the wavenumber in spectra Fig. 2(b) with wavenumbers from 1080 , 956 , and 1180 cm^{-1} indicate an electrostatic interaction between the S=O group and the amine group, resulting in an extension of the S-O bond and a change in the wavenumber toward of

the smaller number. The absorption band at 1459 cm^{-1} corresponds to the asymmetric bend vibration of the methyl group (C-H). At the same time, the asymmetric and symmetrical C-H stretching of the CH_3 group at 2654 and 2916 cm^{-1} showed a long series of alkyl groups in MES, C18. The FTIR absorption band of silica with the addition of the MES template indicated the presence of the appropriate groups. The silica formed shows an absorption peak between $3425\text{ to }3055\text{ cm}^{-1}$ (broad), which was assigned by the stretching OH group (Si-OH), whereas the peak at 956 cm^{-1} was assigned by the asymmetric Si-OH group. The FTIR data is summarized in Table 1.

Other absorption peaks are also observed at $1107\text{ to }1095\text{ cm}^{-1}$ (strong), namely the presence of Si-O-Si groups, and at $804\text{ to }801\text{ cm}^{-1}$, which is caused by the presence of symmetrical Si-O-Si groups [27-28]. In Fig. 2(d), it can be observed that after calcination temperature at $550\text{ }^\circ\text{C}$ still contained organic compounds. The presence of C-H bonds indicates that the template (C18) has not decomposed completely, implying that carbon

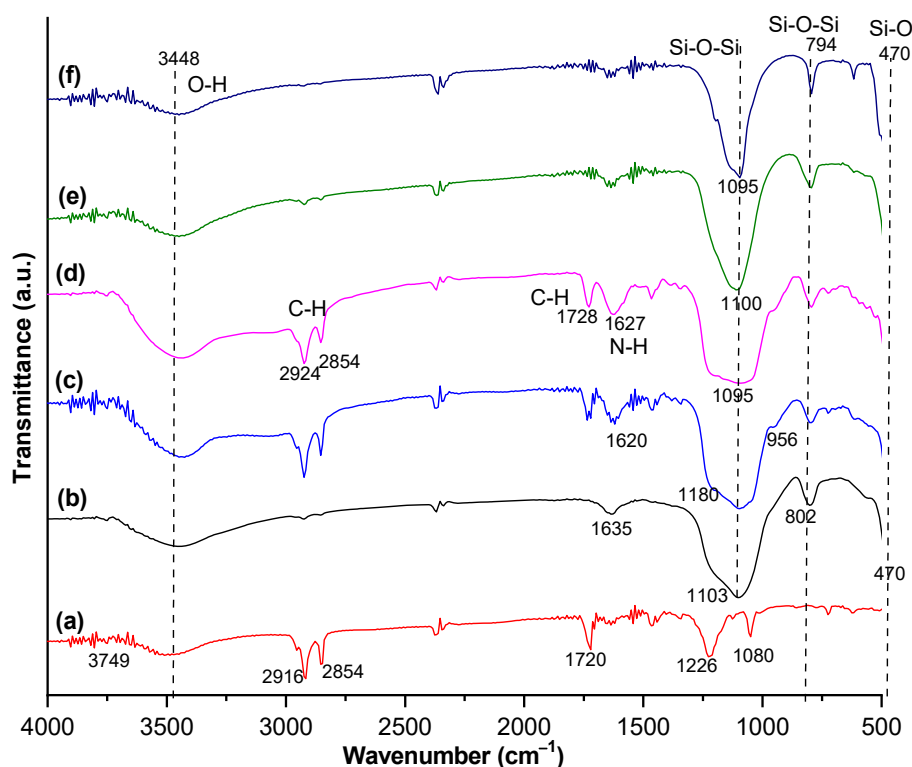


Fig 2. The infrared spectra of (a) MES, (b) SiO_2 , (c) uncalcined $\text{SiO}_2\text{+MES}$, (d) MS-POBA $550\text{ }^\circ\text{C}$, (e) MS-POBA $750\text{ }^\circ\text{C}$, and (f) MS-POBA $950\text{ }^\circ\text{C}$

Table 1. The summary of the FTIR absorption peaks

Wavenumber (cm ⁻¹)	Functional groups
3665–3256	stretching O–H
972	stretching -Si–OH
802	symmetric vibration Si–O
1103	asymmetric vibration Si–O
1080	symmetric S=O
1226	asymmetric S=O
2916–2854	C–H bend in alkane
1720	C=O bending
1599	N–H bending
3378	N–H stretching

atoms are still bonded to hydrogen. To ensure the removal of sulfonate groups in calcination, it can be seen by not showing the wavelength of the sulfonate groups at wavenumbers 1366 to 1015 cm⁻¹ as shown in Fig. 2(e) and 2(f). The carbon component began to disappear after the template had been calcined based on Fig. 2(e) and 2(f), it can be observed that after calcination, there are no peaks visible in the absorption region of 2960 to 2850 cm⁻¹, which is characteristic of asymmetric and symmetric stretching of C–H bonds. This indicates that the template has completely decomposed. This result is related to the

previously confirmed removal of the organic residues that were successfully eliminated through the calcination process since these peaks were not observed in the FTIR spectra [29].

XRD Data

XRD is examined to obtain diffraction patterns of crystalline structures. The XRD pattern of silica material shows a different diffraction pattern, as shown in the diffraction pattern Fig. 3. The pattern of free template silica had a characteristic wide peak at $2\theta = 25.8$ indicating that the material obtained is amorphous [30]. The shape of the wide peak with a peak center around 21–28° indicates that silica was amorphous [4]. The arrangement of atoms in amorphous silica occurs randomly or to a low degree of order. For the MS-POBA material with a calcination temperature template of 750 °C, diffraction peaks experienced a slight shift of 2θ . The first highest peak appeared at 2θ at an angle of 18° and increased crystallinity is marked by the appearance of 2θ values at other peaks, namely 22°, 25°, 27°, 29°, 31°, and 37°. Fig. 3 shows that the crystal phase analysis revealed that the MS-OPBA exhibited multiphase

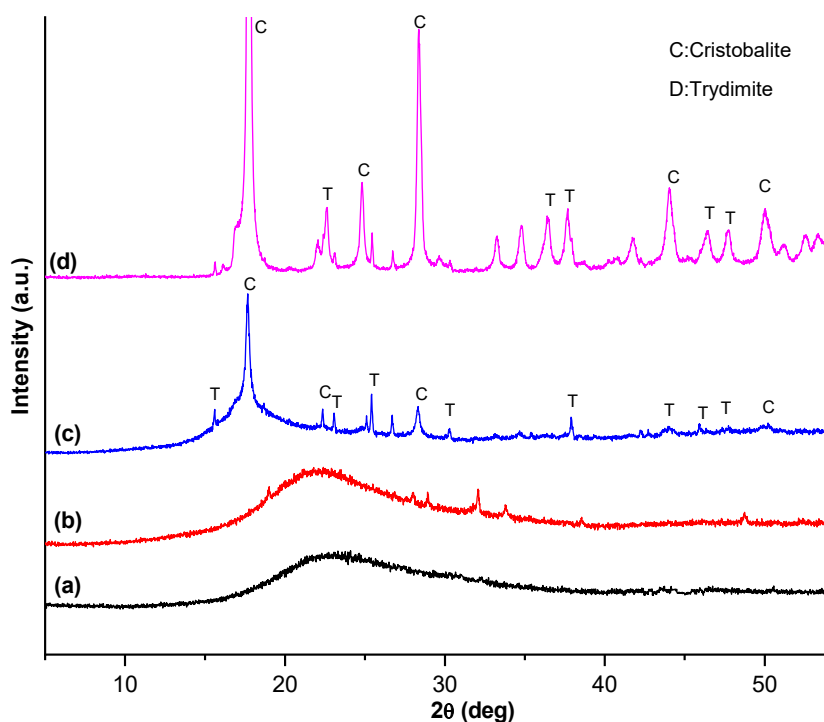


Fig 3. XRD pattern of (a) SiO₂ free template, (b) MS-POBA 550 °C, (c) MS-POBA 750 °C, and (d) MS-POBA 950 °C

characteristics, this finding supports the results from Indrasti et al. [9] with the presence of three distinct crystal phases (quartz, cristobalite, and tridymite) identified under each condition of various temperature calcination.

The MS-POBA with a calcination temperature template of 750 and 950 °C formed a sharp peak, which indicated the crystalline structure of the mesoporous silica material. The diffraction pattern of the silica material at 950 °C shows high peaks and different values and indicates that the silica phase with a crystal structure appears at peaks (2θ) of 17°, 21°, 28°, 31°, 36°, and 43–49°. At higher calcination temperatures, the crystallites formed were larger, which can be attributed to thermally induced crystallite growth [31]. Likewise, MS-POBA with a calcination temperature template of 950 °C shows XRD results similar to MS-POBA at 750 °C. The crystallinity of silica increases with increasing temperature because the structure of silica changes the position of the atoms, which can change as the calcination temperature increases. According to this research, the application of choice is an amorphous material. The advantages of silica from palm oil solid waste are its amorphous form, which makes it more reactive (easier to react), low crystallinity, does not require large processing energy, has a relatively high specific surface area (SSA), economical, and can be easily found.

Surface Analyzer Area BET

To investigate the surface area, pore volume, and pore size of samples, the nitrogen adsorption and desorption isotherm were measured. The BET equation

was used to calculate the isotherm graph and the specific surface area. Pore volume, average pore diameter, and pore size distribution were determined using Barret-Joyner-Halenda (BJH), Isotherm adsorption-desorption analysis of nitrogen at -196 °C was carried out to determine the porosity of a mesoporous silica material. Fig. 4 illustrates the N_2 adsorption/desorption isotherms of the MS-POBA free template and with the template.

The hysteresis curve for the N_2 adsorption-desorption isotherm typically reveals important information about the porous structure of a material. The hysteresis loop is often classified into different types (I, II, III, and IV) based on its shape. The adsorption-desorption isotherm patterns of MS-POBA free template and MS-POBA with templates showed a hysteresis loop in the middle region, which is identical to the type IV adsorption-desorption isotherm according to the IUPAC classification. The type IV curve is associated with the phenomenon of capillary condensation, showcasing a distinctive hysteresis effect characteristic of porous solids [32]. Meanwhile, the N_2 adsorption and desorption isotherms depicted in Fig. 4 for the MS-POBA hysteresis loop observed at $P/P_0 > 0.9$ indicates characteristic materials featuring ink-bottle pores interconnected with narrow necks, typically caused by pore blocking or cavitation [33]. Porous materials are classified according to their pore size into micropores (pore size below 2 nm), mesoporous (pore size between 2 to 50 nm), and macropores (pore size above 50 nm). Specifically, this behavior is indicative of the adsorption type observed in mesoporous (2 to 50 nm).

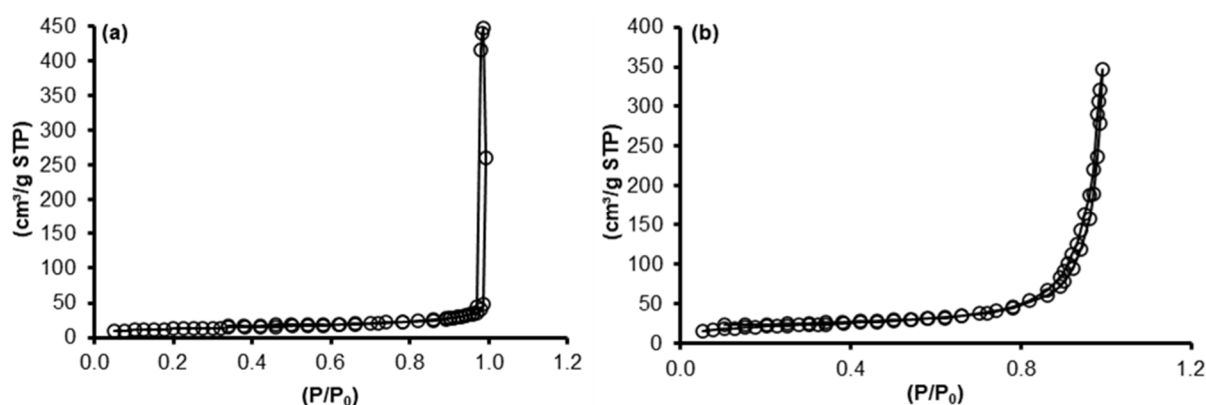


Fig 4. The N_2 adsorption-desorption isotherm of MS-POBA (a) free template and (b) with template

This type of hysteresis loop is characteristic of mesoporous materials with a wide distribution of pore sizes. The loop is wider and exhibits a more pronounced hysteresis, indicating capillary condensation occurring in a range of pore sizes.

The presence of pores on a solid surface caused capillary condensation to occur. This type of pathway is characterized by mesoporous materials [34]. The characteristics of mesoporous silica (MS-POBA) are shown in Table 2. It was found that the N₂ adsorption capacity and the pore size of the samples gradually increased from lower mesopore to upper mesopore when micelles (MES) were used as soft templates. The presence of an anionic surfactant in the micelle as a soft template will enhance the pore diameter significantly from 4.180 to 7.923 nm. This result also showed that the BET surface area of MS-POBA with the template is 71.014 m²/g. This result is not similar to a previous report on mesoporous silica synthesized by using a mixed surfactant template, which showed a much higher surface area (217 m²/g) [18]. However, this research represents a new contribution to the knowledge of anionic surfactants, as no previous studies have reported anionic surfactant MES as the template.

Adsorption Experiments

Silica adsorbs FFA in CPO, supported by the presence of silanol groups to form hydrogen bonds with oxygen from the carbonyl groups in FFAs, as shown in Fig. 5. Oxygen molecules attract hydrogen atoms in the presence of electronegative properties. The presence of polar groups, such as hydroxyl in the adsorbent structure causes them to interact with molecules that have carboxyl groups through hydrogen bonds. The greater number of hydroxyl groups in the adsorbent structure will make its ability to adsorb molecules such as carboxylic acids become greater. In this research, there were two parameters to determine the optimum conditions of adsorption. It is simple, but in this research, we found that the FFA value of CPO is already below the SNI value.

The effect of the adsorbent mass

The increase in mass of the MS-POBA adsorbent is related to the addition of charged sites and hydroxyl groups in the silica structure. It can be a determining factor in the interaction between silica and the carboxyl groups of fatty acids, thus affecting the affinity and adsorption capacity of silica for FFA. The enhancement

Table 2. The surface characters of the adsorbents

Sample	Specific surface area (m ² /g)	Total pore volume (cm ³ /g)	Average pore diameter (nm)
SiO ₂ free template	41.033	0.250	4.180
MS-POBA 550 °C	71.014	0.524	7.923

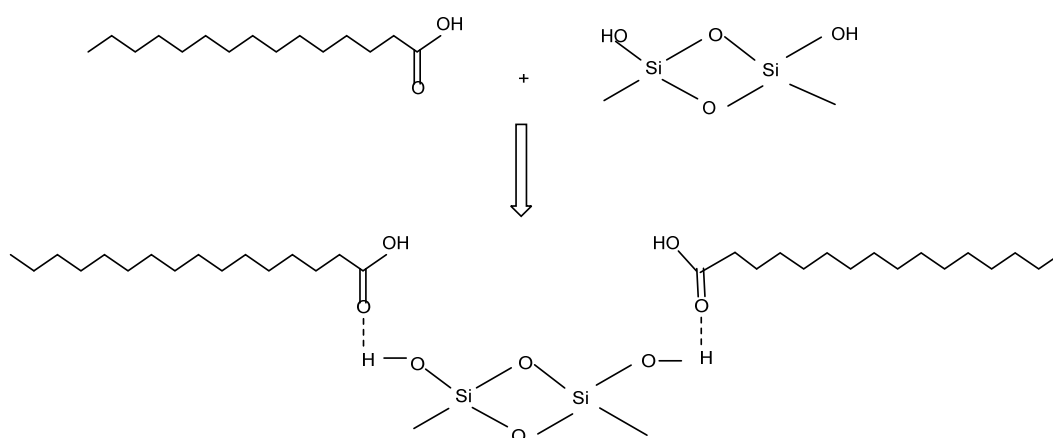


Fig 5. The illustration of the interaction between SiO₂ with FFA

in porosity will give more space that contained in the adsorbent, so that more adsorbates will be adsorbed [35].

Based on Fig. 6, it can be seen that the best reduction occurred at an adsorbent mass of 0.24 g. The increase in the adsorbent dosage indicates a larger surface area and abundance of active sites available to interact with FFA molecules [35]. When the adsorbent dosage was below the optimum value, the removal of FFA was low because of the lower binding sites available for adsorption [36]. The highest percentage removal of FFA was 35.54% compared to MS-POBA without template that only has removal percentage of 26.68%. This result was lower compared to previous research using material adsorbent such as Mg, Ca, Sr, and Ba-based silicate and demonstrated in significant reduction of FFA (> 70%) [37]. This can be due to the high surface area with large adsorption sites of different materials.

The effect of the contact time

Adsorption is a surface process that leads to the transfer of molecules from fluid bulk to solid surface. In this study, the adsorbent was applied to CPO by varying the contact time between them so that the optimum contact time of MS-POBA to adsorb FFA will be known. Based on Fig. 7, the best reduction of FFA by MS-POBA occurred after 20 min of contact time, in which the FFA content was 4.12%.

At the beginning of the process, FFA quickly enters and adsorbed on silica surface because the adsorption sites on the silica surface are still empty. After a further increase in contact time, the adsorption capacity remained almost constant. This indicates that the contact time, MES template MS-POBA, interacts and produces a van der Waals force in the form of a tensile force between the FFA particles and the adsorbent. This process causes FFA to stick to the adsorbent. The adsorption contact time of 20 to 30 min did not result in a significant decrease in the percentage of FFA because the silica surface was almost saturated with FFA compounds. With increasing time, the number of vacant sites decreases, so the adsorption rate is slow. At one point, when the adsorption sites are depleted, there will be repulsion between the adsorbate on the surface of the adsorbent and the adsorbate for FFA [38]. Interestingly, we found that the addition of

adsorbent of MS-POBA free template (4.12%) and MS-POBA with the template (4.68%) onto CPO resulted in the value of FFA having been considered to SNI standard. However, only very limited works reported the MS-POBA material for the removal of FFA in CPO. Recently, Sitinjak [37] used Mg, Ca, Sr, and Ba-based silicate as adsorbent material and further evaluated to find out about the optimum condition of adsorbent MS-POBA. The characteristics of CPO are shown in Table 3.

The adsorption of FFA from CPO on silica shows that adsorption occurs with the formation of a multilayer on the silica surface. The long carbon chains in FFA molecules are nonpolar, making it possible to have an affinity with other nonpolar sides of fatty acid molecules and allow the formation of layers [39].

SEM Data

The characterization of MS-POBA with SEM-EDX was used to determine the 3D surface morphology of the mesoporous silica, as shown in Fig. 8. At 10,000 times

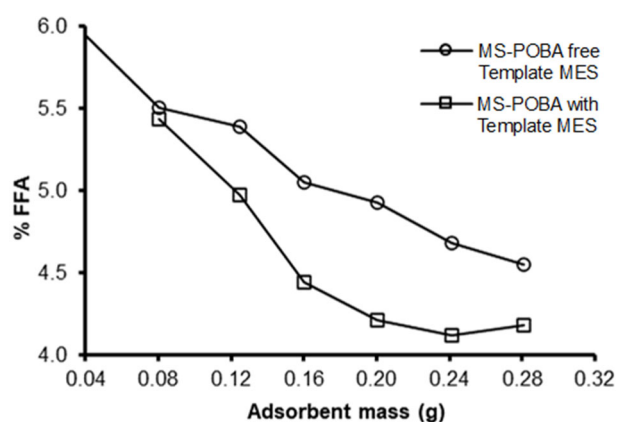


Fig 6. Effects of adsorbent mass

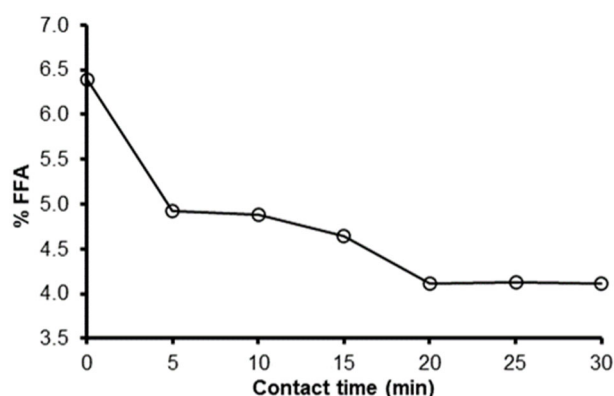
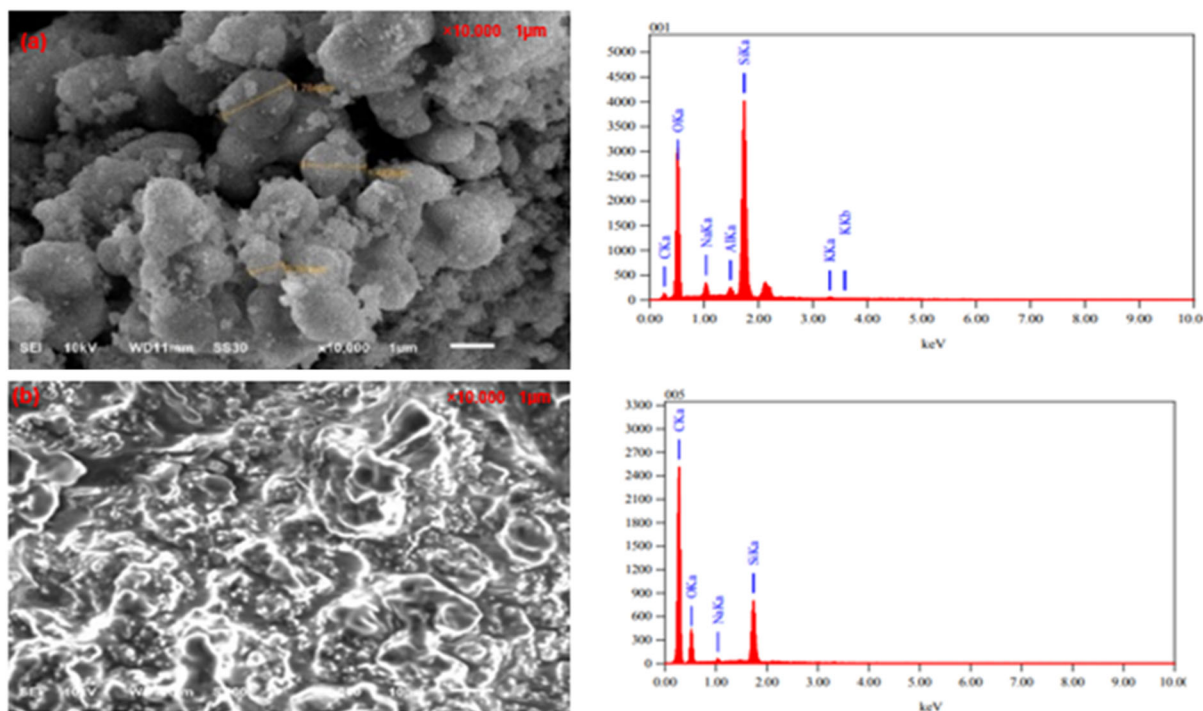


Fig 7. Effects of contact time

Table 3. Characteristic of CPO

Parameter	CPO non-adsorbent (%)	CPO adsorbent free template (%)	CPO adsorbent with template (%)	SNI No 01-2901-2006 (%)
Moisture	0.280	0.138	0.128	0.500
Impurities	0.210	0.204	0.204	0.500
FFA	6.380	4.619	4.108	5.000
Removal		26.68	35.54	

**Fig 8.** SEM for mesoporous materials (a) before and (b) after adsorption

magnification, the MS-POBA material with the MES template obtained had a non-uniform particle distribution, particle size, and hollow particles. The distribution of the particles was small, large, and shaped like a beam with non-uniform sides [30]. Fig. 8(b) shows that the FFAs from CPO filled the empty spaces in the silica material. The elemental composition of the material obtained in this study was 39.90%. Furthermore, the MES template MS-POBA material was used for the adsorption

of fatty acids, and the SEM-EDS results after adsorption are shown in Fig. 8(b).

EDX and mapping observations showed that the nano-silica particle was primarily composed of Si and O (Table 4). Beside Si and O, there were also elements of C and Na. The element with the largest composition from the results of the analysis is element C at 71.45%, followed by the elemental composition of O at around 17.23%, and the mass composition of Si element at 10.95%.

Table 4. The elements of the nano-silica particle based on the EDX test

Element	MS-POBA before adsorption		MS-POBA after adsorption	
	Net weight (wt.%)	Atomic (wt.%)	Net weight (wt.%)	Atomic (wt.%)
C	5.34	8.60	71.45	80.04
O	50.03	60.44	17.23	14.49
Na	2.39	2.01	0.37	0.22
Si	39.90	27.46	10.95	5.25

■ CONCLUSION

In this study, mesopores silica from POBA with the addition of MES as a template and APTMS as co-structure directing agents was successfully synthesized. The alkoxysilane sites of APTMS were co-condensed with silica to form the silica framework. APTMS became positively charged through protonation and subsequently interacted with the negatively charged anionic surfactant (sulfonate group). The mesoporous materials are obtained by subsequent removal of the surfactant by various calcination temperatures where calcination at 550 °C showed that the materials were amorphous, while the crystalline mesoporous materials are obtained at 750 and 950 °C. The BET surface of MS-POBA showed an enhancement by the addition of MES as the template and make it has higher FFA from CPO adsorption ability (35.54%) compared to MS-POBA free template due to its larger surface area.

■ CONFLICT OF INTEREST

The authors declare no known competing financial interests or personal relationships that could have appeared to influence the work reported in this paper.

■ AUTHOR CONTRIBUTIONS

Cita Sitohang: methodology, investigation, data curation, project, and writing. Agus Kuncaka: visualization, validation, and review. Adhitasari Suratman: conceptualization, formal analysis, supervision, review, and editing.

■ REFERENCES

- [1] Anonymous, 2021, *Statistik Kelapa Sawit Indonesia 2021*, BPS - Statistics Indonesia, Jakarta, Indonesia.
- [2] Sequiño, A.C., and Magallon-avenido, J., 2015, The world's leader in the palm oil industry: Indonesia, *IAMURE Int. J. Ecol. Conserv.*, 13, 51–60.
- [3] Bukit, N., Ginting, E.M., Pardede, I.S., Frida, E., and Bukit, B.F., 2018, Mechanical properties of composite thermoplastic HDPE/natural rubber and palm oil boiler ash as a filler, *J. Phys.: Conf. Ser.*, 1120 (1), 012003.
- [4] Ginting, E.M., Bukit, N., Frida, E., and Bukit, B.F., 2020, Microstructure and thermal properties of natural rubber compound with palm oil boilers ash for nanoparticle filler, *Case Stud. Therm. Eng.*, 17, 100575.
- [5] Utama, P.S., Yamsaensung, R., and Sangwichien, C., 2018, Silica gel derived from palm oil mill fly ash, *Songklanakarin J. Sci. Technol.*, 40 (1), 121–126.
- [6] Ginting, E.M., Motlan, M., Bukit, N., Saragih, M.T., Sinaga, A.H., and Frida, E., 2018, Preparation and characterization of oil palm empty bunches powder, *J. Phys.: Conf. Ser.*, 1120 (1), 012004.
- [7] Adha, F.F., 2019, Sintesis Silika dari Abu Boiler Pabrik Kelapa Sawit dengan Variasi Konsentrasi Pelarut NaOH dan Waktu Ekstraksi, *Thesis*, Agro-Industrial Engineering, Faculty of Agricultural Technology, Institut Pertanian Bogor, Indonesia.
- [8] Andrian, R., Ningrum, R.L., and Mardiah, M., 2020, Pembuatan silika dari abu boiler kelapa sawit sebagai katoda udara pada baterai logam udara, *Jurnal Chemurgy*, 4 (2), 24–29.
- [9] Indrasti, N.S., Ismayana, A., Maddu, A., and Utomo, S.S., 2020, Synthesis of nano-silica from boiler ash in the sugar cane industry using the precipitation method, *Int. J. Technol.*, 11, 422–435.
- [10] Schubert, U.S., and Hüsing, N., 2006, *Synthesis of Inorganic Materials*, Wiley-VCH Verlag GmbH & Co, Weinheim, Germany.
- [11] Ubaid, A., Hidayat, N., and Munasir, M., 2017, Aging time effect on porous characteristics of natural mud-based silica prepared by hydrothermal-coprecipitation route, *IOP Conf. Ser.: Mater. Sci. Eng.*, 202 (1), 012022.
- [12] Kubra, K.T., Hasan, M.M., Hasan, M.N., Salman, M.S., Khaleque, M.A., Sheikh, M.C., Rehan, A.I., Rasee, A.I., Waliullah, R.M., Awual, M.E., Hossain, M.S., Alsukaibi, A.K.D., Alshammari, H.M., and Awual, M.R., 2023, The heavy lanthanide of Thulium(III) separation and recovery using specific ligand-based facial composite adsorbent, *Colloids Surf., A*, 667, 131415.
- [13] Rasee, A.I., Awual, E., Rehan, A.I., Hossain, M.S., Waliullah, R.M., Kubra, K.T., Sheikh, M.C., Salman, M.S., Hasan, M.N., Hasan, M.M., Marwani, H.M., Islam, A., Khaleque, M.A., and Awual, M.R., 2023, Efficient separation, adsorption, and recovery

- of Samarium(III) ions using novel ligand-based composite adsorbent, *Surf. Interfaces*, 41, 103276.
- [14] Yokoi, T., and Tatsumi, T., 2007, Synthesis of mesoporous silica materials by using anionic surfactants as template, *J. Jpn. Pet. Inst.*, 50 (6), 299–311.
- [15] Gao, C., Qiu, H., Zeng, W., Sakamoto, Y., Terasaki, O., Sakamoto, K., Chen, Q., and Che, S., 2006, Formation mechanism of anionic surfactant-templated mesoporous silica, *Chem. Mater.*, 18 (16), 3904–3914.
- [16] Han, L., Gao, C., Wu, X., Chen, Q., Shu, P., Ding, Z., and Che, S., 2011, Anionic surfactants templating route for synthesizing silica hollow spheres with different shell porosity, *Solid State Sci.*, 13 (4), 721–728.
- [17] Andriyani, A., 2012, Sintesis Material Mesopori Silika dari Tetraetilortosilikat (TEOS) Menggunakan Natrium Risinoleat sebagai Template dan 3-aminopropiltrimetoksilana (APMS) sebagai Co-Structure Directing Agent (CSDA), *Dissertation*, Department of Chemistry, Faculty of Mathematics and Natural Sciences, Universitas Sumatera Utara, Indonesia.
- [18] Gai, F., Zhou, T., Chu, G., Li, Y., Liu, Y., Huo, Q., and Akhtar, F., 2016, Mixed anionic surfactant-templated mesoporous silica nanoparticles for fluorescence detection of Fe^{3+} , *Dalton Trans.*, 45 (2), 508–514.
- [19] Utama, P.S., Bahri, S., Prawiranegara, B.A., Heltina, D., and Saputra, E., 2022, Synthesis of synthetic amorphous silica powder from palm oil mill fly ash extract by carbon dioxide impregnation, *Mater. Today: Proc.*, 63, S297–S300.
- [20] Wibowo, A.D.K., Yoshi, L.A., Handayani, A.S., and Joelianingsih, J., 2021, Synthesis of polymeric surfactant from palm oil methyl ester for enhanced oil recovery application, *Colloid Polym. Sci.*, 299 (1), 81–92.
- [21] Lin, R., 2016, The Co-Structure Directing Agent (CSDA) Approach to Mesoporous Silica Formation - Exploring the Assembly Characteristics, *Dissertation*, Department of Chemistry, Faculty of Science, Lund University, Sweden.
- [22] Waliullah, R.M., Rehan, A.I., Awual, M.E., Rasee, A.I., Sheikh, M.C., Salman, M.S., Hossain, M.S., Hasan, M.M., Kubra, K.T., Hasan, M.N., Marwani, H.M., Islam, A., Rahman, M.M., Khaleque, M.A., and Awual, M.R., 2023, Optimization of toxic dye removal from contaminated water using chitosan-grafted novel nanocomposite adsorbent, *J. Mol. Liq.*, 388, 122763.
- [23] Ahn, Y., and Kwak, S.Y., 2020, Functional mesoporous silica with controlled pore size for selective adsorption of free fatty acid and chlorophyll, *Microporous Mesoporous Mater.*, 306, 110410.
- [24] Kongnoo, A., Tontisirin, S., Worathanakul, P., and Phalakornkule, C., 2017, Surface characteristics and CO_2 adsorption capacities of acid-activated zeolite 13X prepared from palm oil mill fly ash, *Fuel*, 193, 385–394.
- [25] Porrang, S., Rahemi, N., Davaran, S., Mahdavi, M., and Hassanzadeh, B., 2021, Synthesis of temperature/pH dual-responsive mesoporous silica nanoparticles by surface modification and radical polymerization for anti-cancer drug delivery, *Colloids Surf., A*, 623, 126719.
- [26] Babu, K., Maurya, N.K., Mandal, A., and Saxena, V.K., 2015, Synthesis and characterization of sodium methyl ester sulfonate for chemically-enhanced oil recovery, *Braz. J. Chem. Eng.*, 32 (3), 795–803.
- [27] Al-Abboodi, S.M.T., Al-Shaibani, E.J.A., and Alrubai, E.A., 2020, Preparation and characterization of nano silica prepared by different precipitation methods, *IOP Conf. Ser.: Mater. Sci. Eng.*, 978 (1), 012031.
- [28] Hasanah, M., Sembiring, T., Sebayang, K., Humaidi, S., Rahmadsyah, R., Saktisahdan, T.J., Handoko, F., and Ritonga, S.I., 2021, Extraction of silica dioxide (SiO_2) from mount Sinabung volcanic ash with coprecipitation method, *IOP Conf. Ser.: Mater. Sci. Eng.*, 1156 (1), 012015.
- [29] Shamim, S., Hornyak, G.L., Crespy, D., Kyaw, H., and Bora, T., 2022, Morphology and visible photoluminescence modulation in dye-free

- mesoporous silica nanoparticles using a simple calcination step, *Mater. Res. Bull.*, 152, 111842.
- [30] Barma, M.D., Kannan, S.D., Indiran, M.A., Rajeshkumar, S., and Kumar, R.P., 2020, Antibacterial activity of mouthwash incorporated with silica nanoparticles against *S. aureus*, *S. mutans*, *E. faecalis*: An *in-vitro* study, *J. Pharm. Res. Int.*, 32 (16), 25–33.
- [31] Mitra, J., Ghosh, M., Bordia, R.K., and Sharma, A., 2013, Photoluminescent electrospun submicron fibers of hybrid organosiloxane and derived silica, *RSC Adv.*, 3 (20), 7591–7600.
- [32] Khoeini, M., Najafi, A., Rastegar, H., and Amani, M., 2019, Improvement of hollow mesoporous silica nanoparticles synthesis by hard-templating method via CTAB surfactant, *Ceram. Int.*, 45 (10), 12700–12707.
- [33] Yuan, N., Cai, H., Liu, T., Huang, Q., and Zhang, X., 2019, Adsorptive removal of methylene blue from aqueous solution using coal fly ash-derived mesoporous silica material, *Adsorpt. Sci. Technol.*, 37 (3-4), 333–348.
- [34] Nguyen, N.H., Truong-Thi, N.H., Nguyen, D.T.D., Ching, Y.C., Huynh, N.T., and Nguyen, D.H., 2022, Non-ionic surfactants as co-templates to control the mesopore diameter of hollow mesoporous silica nanoparticles for drug delivery applications, *Colloids Surf., A*, 655, 130218.
- [35] Kepdieu, J.M., Tchanang, G., Njimou, J.R., Djangang, C.N., Maicaneanu, S.A., and Tizaoui, C., 2024, Adsorptive removal of palm oil free fatty acids onto silica-smectite composite: A statistical study using Box–Behnken design in response surface methodology, *Chem. Pap.*, 78 (3), 1775–1790.
- [36] Sheikh, M.C., Hasan, M.M., Hasan, M.N., Salman, M.S., Kubra, K.T., Awual, M.E., Waliullah, R.M., Rasee, A.I., Rehan, A.I., Hossain, M.S., Marwani, H.M., Islam, A., Khaleque, M.A., and Awual, M.R., 2023, Toxic cadmium(II) monitoring and removal from aqueous solution using ligand-based facial composite adsorbent, *J. Mol. Liq.*, 389, 122854.
- [37] Sitinjak, E.M., Masmur, I., Marbun, N.V.M.D., Gultom, G., Sitanggang, Y., and Mustakim, M., 2022, Preparation of Mg, Ca, Sr and Ba-based silicate as adsorbent of free fatty acid from crude palm oil, *Chem. Data Collect.*, 41, 100910.
- [38] Muhdarina, M., Nurhayati, N., Pahlepi, M.R., Pujiana, Z., and Bahri, S., 2019, Penyiapan arang aktif pelepah kelapa sawit sebagai adsorben asam lemak bebas dari CPO (Crude Palm Oil), *al-Kimiya*, 7 (1), 7–13.
- [39] Ayu Putranti, M.L.T., Wirawan, S.K., and Bendiyasa, I.M., 2018, Adsorption of free fatty acid (FFA) in low-grade cooking oil used activated natural zeolite as adsorbent, *IOP Conf. Ser.: Mater. Sci. Eng.*, 299 (1), 012085.